energies

Article

Thermal Effect in Nonlinear One-Dimensional Consolidation of Cold Region Soil

Zongqin Wang [1], Wenbing Wu [1,2], Peng Zhang [1], Zuodong Wang [1], Ruichen Xi [1] and Minjie Wen [2,*]

[1] Faculty of Engineering, China University of Geosciences, Wuhan 430074, China
[2] School of Civil Engineering and Architecture, Zhejiang Sci-Tech University, Hangzhou 310018, China
* Correspondence: 0620577@zju.edu.cn

Abstract: The thermal effect can significantly influence the consolidation of the soil, especially in the cold region. Previous studies have established to research that the drops in the ambient temperature would slow down the consolidation process, resulting in the slow dissipation of excess pore water pressure. In addition, the previous studies neglect the final settlement because consolidation is also influenced by thermal effect. In this paper, a closed-form solution to the one-dimensional nonlinear consolidation of soil considering the thermal effect is proposed. In the mathematical framework, the influences of the thermal effect on the compression index, the permeability, and the elastic modulus of the soil are considered. The solution is fully verified by comparing it with the FDM solution neglecting the thermal effect and the classic Terzaghi's solution. An analysis has been carried out to assess the influence of temperature, stress ratios, consolidation time, the ratio of compression index to permeability index, and the interface parameters on the consolidation process. Different from many previous studies overlooking the thermal effect on the modulus of the soil, a model has been developed which points out that the final settlement due to consolidation would vary significantly with the ambient temperature. Therefore, the thermal effect must be considered in the consolidation calculation of the freeze–thaw cycle soil in the cold region.

Keywords: one-dimensional nonlinear consolidation; thermal effect; closed-form solution; cold region soil; continuous drainage boundary

Citation: Wang, Z.; Wu, W.; Zhang, P.; Wang, Z.; Xi, R.; Wen, M. Thermal Effect in Nonlinear One-Dimensional Consolidation of Cold Region Soil. *Energies* **2022**, *15*, 5643. https://doi.org/10.3390/en15155643

Academic Editor: F. Pacheco Torgal

Received: 10 July 2022
Accepted: 29 July 2022
Published: 4 August 2022

1. Introduction

The thermal effect has a significant influence on the consolidation of the soil [1–3]. Many studies reported that the increase in the temperature would accelerate the consolidation process. The thermal effect on the consolidation of soil in the cold region is often ignored [4,5]. The cold environment would not only slow down the consolidation of the cold region soil but also result in different consolidation-induced final settlements. Hence, it is essential to establish the fundamental consolidation theory to guide the consolidation analysis of the cold region soil [6–8].

Many publications can be found referring to the thermal effect on soil consolidation. For instance, Paaswell [9] found that the consolidation-induced settlement can vary differently with the temperature through experimental studies. Subsequently, Drnevich et al. [10] compared the temperature effect on pre-consolidation between the model test and field test. Booker and Savvidou [11] investigated the heat source based on Biot's theories, which would cause the pore water pressure to dissipate. Later, an analytical solution was developed to solve the problem of a point heat source buried deep [12,13]. The scholars proposed the foundation treatment technology by thermal consolidation [14–17]. Meanwhile, an experimental test was carried out to justify the thermal effects on the mechanical [18]. Despite the influence of temperature on the soil constitutive model, it is necessary to investigate a half-space subjected to thermal loading [19]. Bai [20] introduced the thermos-osmosis effect and thermal filtration effect of saturated porous half-space under the variable thermal loading. Chen and Ledesma [21] used Laplace transform domain to solve the coupled T-H problem in the unsaturated clay barrier. Yu and Chen [22] investigated the importance of the coupled effect of thermally driven moisture transport that can alter the flow field in the low-permeability medium. Ai and Wang [23] applied the Laplace-Hankel transform to obtain an analytical layer element solution of the governing equations which considered axisymmetric thermal consolidation in multilayered porous thermoelastic media.

In addition to the thermal effect, the soil constitutive model and boundary conditions are also key factors influencing the consolidation process. Since Terzaghi [24] established the theory of one-dimensional linear consolidation based on Darcy's law, scholars carried out a lot of research work on the load forms, the soil constitutive model, and drainage boundaries to satisfy various practical cases. Davis and Raymond [25] introduced the assumption that the soil permeability coefficient is constant to simplify the mathematical work. Based on the assumption, a closed-form solution was derived to solve the governing equation of the one-dimensional nonlinear consolidation which contains the logarithmic relationship between void ratio and effective stress. Chen et al. [26] further developed the layered nonlinear consolidation. Researchers proposed various solutions to incorporate the conditions e.g., layered soils under variable loading and ramp loading [27–29]. However, the consolidation coefficient did not always remain constant for most engineering scenes. Mesri and Rokhsar [30] developed nonlinear consolidation based on the assumption including the logarithmic relationship among void ratio, effective stress, and permeability coefficient. Subsequently, the scholars obtained different solutions through different methods such as the finite element method (FEM) and differential quadrature method (DQM) [31–33]. All these solutions are based on the Terzaghi drainage boundary [24]. It regarded the boundaries as fully permeable or impermeable. However, the real drainage surface lies between the permeable and the impermeable boundaries. To authentically model the drainage boundary conditions, Gay [34] developed the impeded drainage boundary. Schiffman and Stein [35] focused on the changes in soil permeability and compressibility with impeded drainage boundaries. Mesri [36] developed a closed-form solution to one-dimensional linear consolidation based on the impeded drainage boundary. It is complicated to solve the governing equation based on the nonlinear consolidation theory with impeded drainage boundary. Mei et al. [37,38] proposed the continuous drainage boundary that is convenient to obtain a closed-form solution. Zhou et al. [39] and Wang [40] introduced the continuous boundary into the unsaturated soil to obtain a semi-analytical solution. Huang et al. [41] further developed two-dimensional consolidation of unsaturated soil. Zong et al. [42] utilized the finite difference method to obtain the solution of one-dimensional nonlinear consolidation based on continuous drainage boundary.

In summary, the above-mentioned studies fail to reveal the authentic one-dimensional nonlinear consolidation considering the negative thermal effect. Hence, it is necessary to establish a rigorous nonlinear mathematical framework to guide the consolidation analysis of the soil in the cold region.

2. Mathematical Model and Assumptions

2.1. Mathematical Model

The mathematical model established is depicted in Figure 1. Only the soil deformation and the water flow that occurred in the vertical direction are considered. To account for the thermal effect, the relationships between the compressibility and permeability of the soil and the ambient temperature are considered. The surcharge load is uniformly subjected at the ground surface.

2.2. General Assumptions

The main assumption adopted in the present study are listed as

(1) The soil is homogeneous, isotropic and fully saturated.
(2) The volumes of soil particles are incompressible.
(3) The deformation of the soil caused by the consolidation is small.

(4) The seepage flow of pore water inside the soil obeys Darcy's law.
(5) The drainage condition is modeled by the continuous drainage boundary.

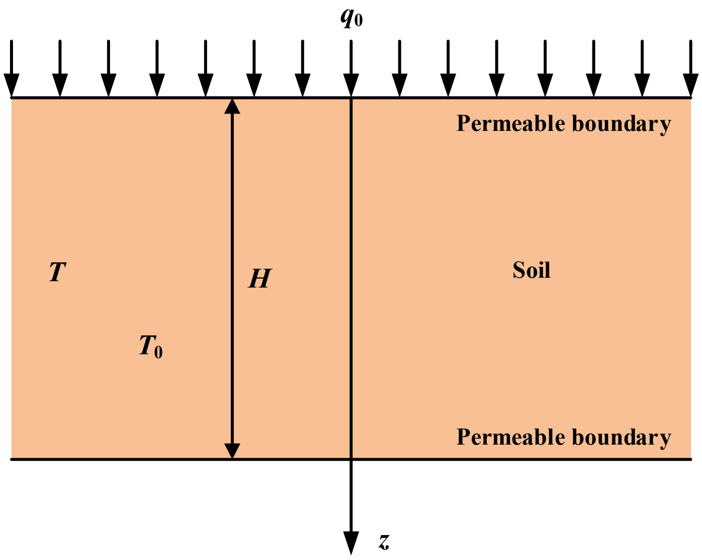

Figure 1. Schematic diagram of one-dimensional consolidation model.

3. Governing Equations and Solutions

3.1. Governing Equation

According to Quan et al. [43], the empirical formula for the compression index can be expressed as

$$C_c = A + \chi \frac{T}{T_0} \tag{1}$$

where, T is the temperature, $T_0 = 20$ °C. According to the field tests by Eriksson et al. [44], A and χ are constants, which are related to the tests.

According to Mesri and Rokhsar [30], the void ratio change due to the variation of effective stress is

$$e = e_0 - C_c \lg \frac{\sigma'}{\sigma'_0} \tag{2}$$

$$e = e_0 + C_k \lg \frac{k_v}{k_{v0}} \tag{3}$$

where, e_0 is initial void ratio. σ' and σ'_0 are effective stress and initial effective stress, respectively. C_k represents the penetration index. k_v and k_{v0} represent the permeability coefficient and initial the permeability coefficient, respectively.

Substitution Equation (1) into Equation (2), yields

$$e = e_0 - \left(A + \chi \frac{T}{T_0} \right) \lg \frac{\sigma'}{\sigma'_0} \tag{4}$$

According to Wang et al. [45], the relationship between the permeability coefficient and the dynamic viscosity coefficient of water is

$$k_{vT} = k_{vR} \frac{\eta_R}{\eta_T} \tag{5}$$

where, k_{vR} is the permeability coefficient at temperature R $= 20$ °C. η_R and η_T are the dynamic viscosity coefficients of water at temperature T and R, respectively.

According to Guo et al. [46], the relationship between the dynamic viscosity coefficient of water and the temperature is linear, which can be given as

$$\frac{\eta_{\mathrm{R}}}{\eta_{\mathrm{T}}} = \frac{T + T_0}{2T_0} \tag{6}$$

Substituting Equation (6) into Equation (5), yields

$$k_{\mathrm{v}T} = k_{\mathrm{vR}} \frac{T + T_0}{2T_0} \tag{7}$$

According to Mesri and Rokhsar [30], one can obtain

$$k_{\mathrm{vR}} = k_{\mathrm{v0}} \left(\frac{\sigma'_0}{\sigma'} \right)^{\frac{C_{\mathrm{c}}}{C_{\mathrm{k}}}} \tag{8}$$

Substituting Equation (8) into Equation (7), yields

$$k_{\mathrm{v}T} = \frac{T + T_0}{2T_0} k_{\mathrm{v0}} \left(\frac{\sigma'_0}{\sigma'} \right)^{\frac{C_{\mathrm{c}}}{C_{\mathrm{k}}}} \tag{9}$$

The consolidation coefficient can be expressed as

$$C_{\mathrm{v}} = \frac{k_{\mathrm{v}T}}{m_{\mathrm{v}} \gamma_{\mathrm{w}}} \tag{10}$$

According to Darcy's law, the seepage is

$$v = k_{\mathrm{v}} i = -\frac{k_{\mathrm{v}T}}{\gamma_{\mathrm{w}}} \frac{\partial u}{\partial z} \tag{11}$$

where, γ_{w} is the unit weight of water, and u presents the excess pore water pressure. z is the variable of space in the vertical direction.

Substituting Equation (9) into Equation (11) yields

$$\frac{\partial v}{\partial z} \mathrm{d}z = -\frac{\partial}{\partial z} \left[\frac{T + T_0}{2T_0} \left(\frac{\sigma'_0}{\sigma'} \right)^{\frac{C_{\mathrm{c}}}{C_{\mathrm{k}}}} \frac{k_{\mathrm{v0}}}{\gamma_{\mathrm{w}}} \frac{\partial u}{\partial z} \right] \mathrm{d}z \tag{12}$$

According to assumption (1), $V_{\mathrm{v}} = V_{\mathrm{w}}$; thus

$$\frac{\partial V_{\mathrm{w}}}{\partial t} = -\frac{\partial}{\partial t} \left(\frac{e}{1 + e_0} \mathrm{d}x \mathrm{d}y \mathrm{d}z \right) \tag{13}$$

Based on the relationship between the strain and stress, it can be expressed as

$$v = k_{\mathrm{v}} i = -\frac{k_{\mathrm{v}T}}{\gamma_{\mathrm{w}}} \frac{\partial u}{\partial z} \tag{14}$$

Substituting Equation (14) into Equation (13), yields

$$\frac{\partial V_{\mathrm{w}}}{\partial t} = \frac{0.434 C_{\mathrm{c}}}{(1 + e_1)\sigma'} \frac{\partial \sigma'}{\partial t} \mathrm{d}x \mathrm{d}y \mathrm{d}z \tag{15}$$

The reduction in pore volume in the soil unit is equal the amount of water flowing out the unit.

$$\frac{\partial V_{\mathrm{w}}}{\partial t} \mathrm{d}t = \frac{\partial v}{\partial z} \mathrm{d}x \mathrm{d}y \mathrm{d}z \mathrm{d}t \tag{16}$$

Combining Equations (15) and (16), yields

$$\frac{\partial v}{\partial z} = \frac{0.434 C_{\mathrm{c}}}{(1 + e_1)\sigma'} \frac{\partial \sigma'}{\partial t} \tag{17}$$

Substituting Equation (17) into Equation (12), one obtains

$$\frac{0.434C_c}{(1+e_0)\sigma'}\frac{\partial\sigma'}{\partial t}=-\frac{\partial}{\partial z}\left(\frac{T+T_0}{2T_0}\left(\frac{\sigma'_0}{\sigma'}\right)^{\frac{C_c}{C_k}}\frac{k_{v0}}{\gamma_w}\frac{\partial u}{\partial z}\right) \tag{18}$$

According to the principle of the effective stress, the thermal consolidation equation can be expressed as

$$\frac{\partial u}{\partial t}=\frac{\partial}{\partial z}\left(\frac{T+T_0}{2T_0}c_{v0}\left(\frac{\sigma'}{\sigma'_0}\right)^{1-\frac{C_c}{C_k}}\frac{\partial u}{\partial z}\right) \tag{19}$$

where, $c_{v0}=\frac{k_{v0}(1+e_0)\sigma'_0}{0.434C_c\gamma_w}$.

3.2. Boundary Conditions

(1) The upper and bottom boundary conditions are modelled by the continuous drainage boundary:

$$z=0, u=q_0 e^{-\alpha\frac{c_{v0}}{H}t} \tag{20}$$

$$z=H, u=q_0 e^{-\beta\frac{c_{v0}}{H}t} \tag{21}$$

where, q_0 is the surcharge load. α and β are the interface parameters, which are related to the permeability of the soil [37,38]. H is the thickness of the soil.

(2) The initial condition can be express as

$$t=0, u=q_0 \tag{22}$$

3.3. Approximate Solutions for the Governing Equations

In order to facilitate the mathematical derivation, the following assumption is introduced

$$\omega=\left(N_q\right)^{1-\frac{C_c}{C_k}}-\left(\frac{\sigma'}{\sigma'_0}\right)^{1-\frac{C_c}{C_k}} \tag{23}$$

Substituting Equation (22) into Equation (19), yields

$$\frac{\partial\omega}{\partial t}=\frac{T+T_0}{2T_0}c_{v0}\omega\frac{\partial^2\omega}{\partial z^2} \tag{24}$$

The dimensionless parameters are introduced herein as:

$$T_v=\frac{c_{v0}}{H^2}t=\frac{B}{(A+\chi T/T_0)H^2}t, Z=\frac{z}{H}, \overline{u}=\frac{u}{q_0} \tag{25}$$

where, $B=\frac{k_{v0}(1+e_0)\sigma'_0}{0.434\gamma_w}$.

Substituting Equation (25) into Equation (24), ω is replaced by the mean ω_0.

$$\frac{\partial\omega}{\partial T_v}=\frac{T+T_0}{2T_0}\omega_0\frac{\partial^2\omega}{\partial Z^2} \tag{26}$$

where, $\omega_0=\frac{1}{2}\left[1+N_q{}^{1-\frac{C_c}{C_k}}\right]$ [47].

The boundary condition can satisfy

$$T_v=0, \omega=\left(N_q\right)^{1-\frac{C_c}{C_k}}-1 \tag{27}$$

$$Z=0, \omega=\omega_\alpha(T_v) \tag{28}$$

$$Z=1, \omega=\omega_\beta(T_v) \tag{29}$$

where $\omega_\alpha(t) = (N_\mathrm{q})^{1-\frac{C_\mathrm{c}}{C_\mathrm{k}}} - \left[N_\mathrm{q} - (N_\mathrm{q}-1)\mathrm{e}^{-\alpha T_\mathrm{v}}\right]^{1-\frac{C_\mathrm{c}}{C_\mathrm{k}}}$,
$\omega_\beta(t) = (N_\mathrm{q})^{1-\frac{C_\mathrm{c}}{C_\mathrm{k}}} - \left[N_\mathrm{q} - (N_\mathrm{q}-1)\mathrm{e}^{-\beta T_\mathrm{v}}\right]^{1-\frac{C_\mathrm{c}}{C_\mathrm{k}}}$.

After homogenizing the boundary conditions, one obtains

$$\omega = v + Z\left[\omega_\beta(T_\mathrm{v}) - \omega_\alpha(T_\mathrm{v})\right] + \omega_\alpha(T_\mathrm{v}) \tag{30}$$

Substituting Equation (30) into Equation (26), yields

$$\frac{\partial v}{\partial T_\mathrm{v}} = \frac{T+T_0}{2T_0}\omega_0\frac{\partial^2 v}{\partial Z^2} + f(Z, T_\mathrm{v}) \tag{31}$$

where,

$$f(Z, T_\mathrm{v}) = Z\left(\frac{\mathrm{d}\omega_\beta(T_\mathrm{v})}{\mathrm{d}T_\mathrm{v}} - \frac{\mathrm{d}\omega_\alpha(T_\mathrm{v})}{\mathrm{d}T_\mathrm{v}}\right) + \frac{\mathrm{d}\omega_\alpha(T_\mathrm{v})}{\mathrm{d}T_\mathrm{v}} \tag{32}$$

$$\frac{\mathrm{d}\omega_\beta(T_\mathrm{v})}{\mathrm{d}T_\mathrm{v}} = -\beta D\mathrm{e}^{-\beta T_\mathrm{v}}\left[1 + \sum_{m=1}^{\infty} C_m \mathrm{e}^{-\beta m T_\mathrm{v}}\right] \tag{33}$$

$$\frac{\mathrm{d}\omega_\alpha(T_\mathrm{v})}{\mathrm{d}T_\mathrm{v}} = -\alpha D\mathrm{e}^{-\alpha T_\mathrm{v}}\left[1 + \sum_{m=1}^{\infty} C_m \mathrm{e}^{-\alpha m T_\mathrm{v}}\right] \tag{34}$$

$$D = \left(1 - \frac{C_\mathrm{c}}{C_\mathrm{k}}\right)(N_\mathrm{q}-1)(N_\mathrm{q})^{-\frac{C_\mathrm{c}}{C_\mathrm{k}}} \tag{35}$$

$$C_m = \frac{(-1)^m}{m!}\left(1 - \frac{1}{N_\mathrm{q}}\right)^m\left(-\frac{C_\mathrm{c}}{C_\mathrm{k}}\right)\left(-\frac{C_\mathrm{c}}{C_\mathrm{k}} - 1\right)\cdots\left(-\frac{C_\mathrm{c}}{C_\mathrm{k}} - m + 1\right) \tag{36}$$

The initial and boundary conditions are

$$v(0, Z) = 0 \tag{37}$$

$$v(0, T_\mathrm{v}) = 0 \tag{38}$$

$$v(1, T_\mathrm{v}) = 0 \tag{39}$$

According to the intrinsic function system, the solution of the Equation (31) can be expressed as

$$v(Z, T_\mathrm{v}) = \sum_{n=1}^{\infty} v_n(T_\mathrm{v})\sin(n\pi Z) \tag{40}$$

Substituting Equation (39) into Equation (30), yields

$$\sum_{n=1}^{\infty} v'_n(T_\mathrm{v})\sin(n\pi Z) - \sum_{n=1}^{\infty} f_n(T_\mathrm{v})\sin(n\pi Z) = -(n\pi)^2\frac{\mathrm{T}+\mathrm{T}_0}{2\mathrm{T}_0}\omega_0\sum_{n=1}^{\infty} v_n(T_\mathrm{v})\sin(n\pi Z) \tag{41}$$

where, $f_n(T_\mathrm{v}) = 2\int_0^1 f(Z, T_\mathrm{v})\sin(n\pi Z)\mathrm{d}Z$.

In other words:

$$v'_n(T_\mathrm{v}) + f'_n(T_\mathrm{v}) + (n\pi)^2\frac{T+T_0}{2T_0}\omega_0 v_n(T_\mathrm{v}) = 0 \tag{42}$$

Subsequently, applying Laplace transform to Equation (42), one obtains

$$sv_n(s) + (n\pi)^2 M v_n(s) = F_n(s) \tag{43}$$

where, $M = \frac{T+T_0}{2T_0}\omega_0$, $L[v'_n(T_\mathrm{v})] = sv_n(s) - v_n(0) = sv_n(s)$, $L[v_n(T_\mathrm{v})] = v_n(s)$, $L[f_n(T_\mathrm{v})] = F_n(s)$, $L[\,]$ represents the Laplace transform.

Obviously, the Equation (43) can be expressed as

$$v_n(s) = \frac{F_n(s)}{s + (n\pi)^2 M} \tag{44}$$

Incorporating inverse Laplace transform into Equation (44), one can obtain

$$\begin{aligned} v_n(T_\mathrm{v}) = {} & -2\frac{(-1)^{n-1}}{n\pi}\beta D\frac{\mathrm{e}^{-\beta T_\mathrm{v}} - \mathrm{e}^{-(n\pi)^2 M T_\mathrm{v}}}{(n\pi)^2 M - \beta} - 2\frac{(-1)^{n-1}}{n\pi}\beta D\sum_{m=1}^{\infty} C_m \frac{\mathrm{e}^{-\beta(m+1)T_\mathrm{v}} - \mathrm{e}^{-(n\pi)^2 M T_\mathrm{v}}}{(n\pi)^2 M - (m+1)\beta} \\ & - \frac{2}{n\pi}\alpha D\frac{\mathrm{e}^{-\alpha T_\mathrm{v}} - \mathrm{e}^{-(n\pi)^2 M T_\mathrm{v}}}{(n\pi)^2 M - \alpha} - \frac{2}{n\pi}\alpha D\sum_{m=1}^{\infty} C_m \frac{\mathrm{e}^{-\alpha(m+1)T_\mathrm{v}} - \mathrm{e}^{-(n\pi)^2 M T_\mathrm{v}}}{(n\pi)^2 M - (m+1)\alpha} \end{aligned} \tag{45}$$

Substituting Equations (45) and (30) into Equation (23), the dimensionless excess pore water pressure can be expressed as

$$u = {\sigma'}_\mathrm{f} - {\sigma'}_0\left[\left(N_q\right)^{1-\frac{C_\mathrm{c}}{C_\mathrm{k}}} - v\right]^{\frac{C_\mathrm{k}}{C_\mathrm{k}-C_\mathrm{c}}} \tag{46}$$

According to the empirical formula by Li et al. [48], the relationship between the elastic modulus, the temperature, and the strain rate can be expressed by the following equation.

$$E = (153.59|T| + 766.53)\cdot(\varepsilon/\varepsilon_0)^m \tag{47}$$

where, ε and $\varepsilon_0 = 1s^{-1}$ represent the strain rate and the dimensionless reference strain rate, respectively. m is the empirical parameter. When $-15\ ^\circ\mathrm{C} \le T \le -2\ ^\circ\mathrm{C}$, $m = 0.178$. Therefore, the soil consolidation settlement can be expressed as:

$$s = \frac{\int_0^H u_0 - u_t \mathrm{d}z}{(153.59|T| + 766.53)\cdot(\varepsilon/\varepsilon_0)^{0.178}} \tag{48}$$

The average degree of consolidation defined by excess pore water pressure can be established as:

$$U_\mathrm{p} = 1 - \int_0^1 \frac{u}{q_0}\mathrm{d}Z \tag{49}$$

The average degree of consolidation defined by settlement can be expressed as:

$$U_\mathrm{s} = \frac{\int_0^H \varepsilon \mathrm{d}z}{\int_0^H \varepsilon_\mathrm{f} \mathrm{d}z} \tag{50}$$

where, $\varepsilon = \frac{C_{cT}}{1+e_0}\lg\left(\frac{\sigma'}{{\sigma'}_0}\right)$ and $\varepsilon_\mathrm{f} = \frac{C_{cT}}{1+e_0}\lg\left(\frac{{\sigma'}_\mathrm{f}}{{\sigma'}_0}\right)$ are the soil strain and the maximum soil strain in vertical direction.

4. Model Verifications

4.1. Comparisons with the Solution by Quan et al.

In this section, the present solution is compared with the solution based on the Terzaghi boundary. As the interface parameters approach infinity ($\alpha = \beta = 10{,}000$), the continuous drainage boundary can be degenerated into Terzaghi drainage boundary.

$$Z = 0,\ \omega = \omega_\alpha(T_\mathrm{v}) = 0 \tag{51}$$

$$Z = 1,\ \omega = \omega_\beta(T_\mathrm{v}) = 0 \tag{52}$$

$$v_n(T_\mathrm{v}) = \left[\frac{2}{n\pi} - 2\frac{(-1)^{n-1}}{n\pi}\right]\left({N_\mathrm{q}}^{1-\frac{C_\mathrm{c}}{C_\mathrm{k}}} - 1\right)\mathrm{e}^{-(n\pi)^2 M T_\mathrm{v}} \tag{53}$$

Substituting Equation (53) into Equation (30), based on the Terzaghi double-sided drainage boundary, the ω can be obtained as

$$\omega = N_{\mathrm{q}}{}^{1-\frac{C_{\mathrm{c}}}{C_{\mathrm{k}}}} - \left(N_{\mathrm{q}}{}^{1-\frac{C_{\mathrm{c}}}{C_{\mathrm{k}}}} - 1\right)\sum_{n=1,3,5\cdots}^{\infty} \frac{4}{n\pi}\sin(n\pi Z)\mathrm{e}^{-(n\pi)^2 M T_{\mathrm{v}}} \tag{54}$$

Replacing the H in the double-sided drainage with $2H$, the consolidation corresponding to the Terzaghi drainage condition can be obtained as

$$\omega = N_{\mathrm{q}}{}^{1-\frac{C_{\mathrm{c}}}{C_{\mathrm{k}}}} - \left(N_{\mathrm{q}}{}^{1-\frac{C_{\mathrm{c}}}{C_{\mathrm{k}}}} - 1\right)\sum_{n=1}^{\infty} \frac{4}{(2n-1)\pi}\sin\left(\frac{(2n-1)\pi}{2}Z\right)\mathrm{e}^{-\left(\frac{(2n-1)\pi}{2}\right)^2 M T_{\mathrm{v}}} \tag{55}$$

During the comparison with the solution by Quan et al. [43], $C_{\mathrm{c}}/C_{\mathrm{k}} = 1$. In addition, the effect of temperature on the soil compressive modulus is not considered. According to the test by Eriksson et al. [44], the soil parameters are provided in Table 1. Unless otherwise stated, the soil parameters remain the same in the following paragraphs.

Table 1. Soil profiles given by Eriksson [44].

A	χ	H (m)	k_{v0} (m/s)	σ'_0 (kPa)	σ'_f (kPa)	e_0
0.275	0.005	1	10^{-8}	1	101	1.2

A comparison of consolidation degree defined by settlement between the degenerated solution and the solution by Quan et al. [43] is shown in Figure 2. Generally, the present degradation is in good fitness with the solution by Quan et al. [43]. But the continuous drainage boundary can reflect the change of excess pore water pressure on the ground. With the increase of the temperature, the consolidation rate and the dissipation of the excess pore water pressure would increase and be accelerated.

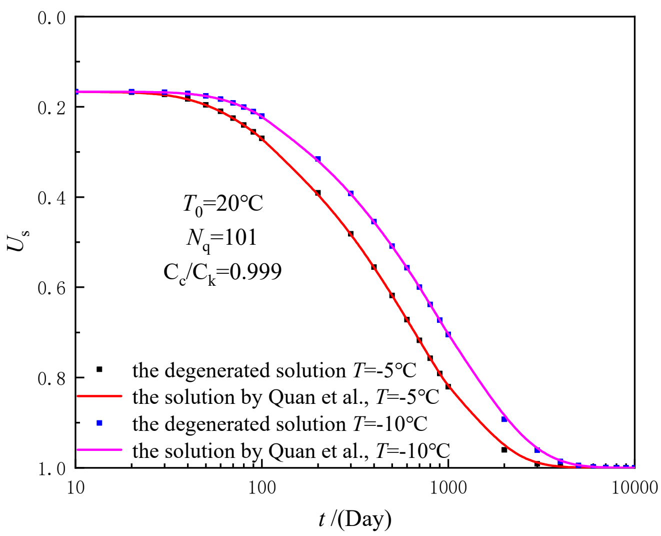

Figure 2. Comparisons between the solution by Quan et al. [43] and the present degradation solution.

4.2. Comparisons with the Finite Difference Solution Neglecting the Thermal Effect

To verify the rationality of the present solution, the present solution is compared with the finite difference method by Zong et al. [42], in which the thermal effect is neglected. When T is equal to $T_0 = 20$ °C, the present solution is degenerated, which means that the compressibility coefficient and permeability coefficient of the soil decrease with the decrease of the void ratio. As shown in Figure 3, the degree of consolidation defined by excess pore water pressure in present solution is in good agreement with the finite difference solution, which justifies the reliability of the present solution. It is also observed that the dissipation of the excess pore water pressure would slow down with the increase of $C_{\mathrm{c}}/C_{\mathrm{k}}$.

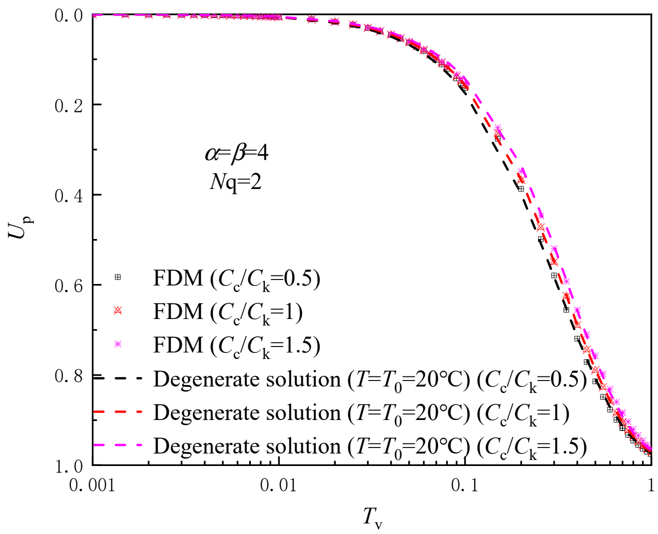

Figure 3. Comparisons between the finite difference solution and the present degradation.

5. Parametric Study

To further analyze the parameters related to the model proposed by this study, a parametric study is conducted. The soil adopted herein is listed in Tabs. 1 given by Eriksson [44].

5.1. Influence of Temperature

The ambient temperature around the soil can be different at different cold regions. Therefore, it is necessary to analyze the effect on the consolidation rate under different temperature conditions. As shown in Figure 4, it presents the influence of the temperature on the excess pore water pressure and the degree of the consolidation defined by the settlement and excess pore water pressure. The growth of the temperature would increase the dissipation rate of excess pore water pressure. As the temperature increases, the compressibility index of the soil would increase, because of which the permeability of the soil would also increase. The temperature has a greater effect on the dissipation of excess pore water pressure as shown in Figure 4a. Although the time is the same, the excess pore water pressure of the drainage interface is different. This is because the temperature has an influence on the initial consolidation coefficient, resulting in an incompletely aligned drainage boundary. It is also interesting to find that the effect of temperature on the dissipation of pore pressure is especially pronounced at low temperature ($T < T_0 = 20$ °C).

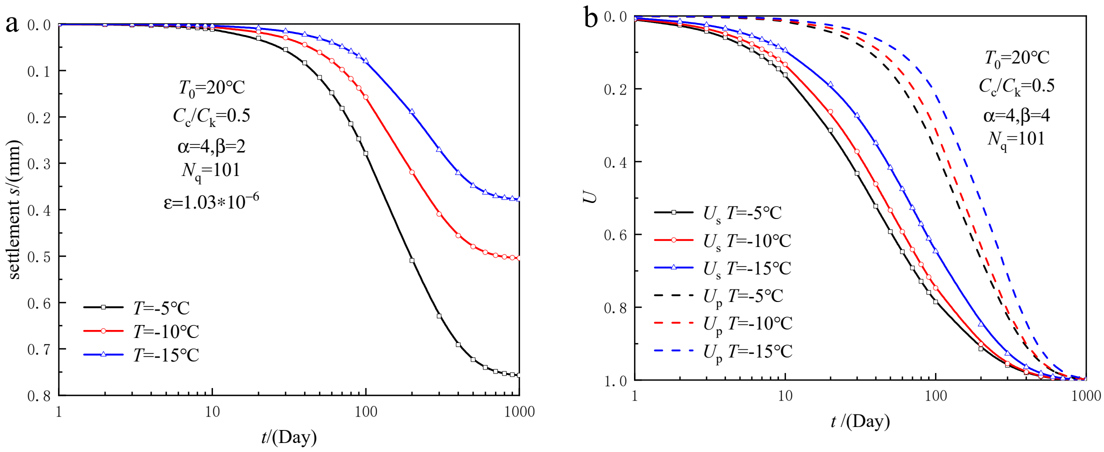

Figure 4. Influence of the temperature: (**a**) the distribution of the settlement, and (**b**) the distribution of the degree of the consolidation defined by settlement and excess pore water pressure.

5.2. Influence of the Ratio of Finial Effective Stress to Initial Effective N_q

Figure 5 depicts the distribution of the excess pore water pressure along the depth. The permeability coefficient of the soil k_v and the compress coefficient of the soil m_v would decrease with the increase of N_q. When $C_c/C_k < 1$, k_v decreases slower than m_v. Therefore, the main factor influencing the soil consolidation rate is the compressive modulus. The smaller the m_v, the harder the soil is to compress, that makes the rate of the soil settling slow. When the ratio of the compress index to permeability index C_c/C_k is less than 1, the pore pressure dissipation rate increases as N_q increases. However, the opposite occurs when $C_c/C_k > 1$. With the increase of N_q, the excess pore water pressure would increase under the same boundary conditions. That is because k_v is the main factor to change the dissipation of excess pore water pressure during consolidation when $C_c/C_k > 1$. The increase in permeability would accelerate the dissipation of excess pore water pressure.

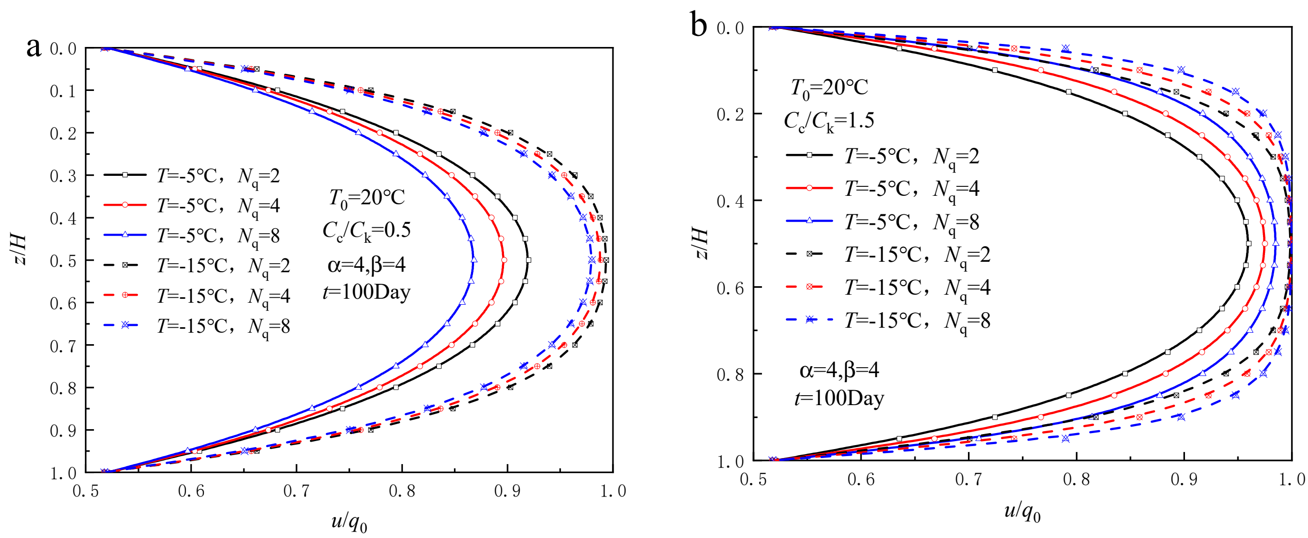

Figure 5. Influence of N_q: (**a**) the distribution of excess pore water pressure ($C_c/C_k < 1$), and (**b**) the distribution of excess pore water pressure ($C_c/C_k > 1$).

5.3. Influence of Time

Figure 6 presents the relationship between the distribution of excess pore water pressure and the consolidation time. The excess pore water pressure would decrease dramatically with the increase in time at the drainage boundary, that is one of the biggest differences from the Terzaghi drainage boundary. As is shown in Figure 6a, when $\alpha = \beta$, under which circumstance the ground surface and the bottom surface of the soil have the same permeability, the distribution of excess pore water pressure is symmetrical in the depth of the soil layer. The increase in time would only result in the decrease of excess pore water pressure amplitudes. The average excess pore water pressure in the upper side of the soil is significantly lower than that in the lower when $\alpha > \beta$, which is suggested by Figure 6b. It is evident that the permeability of the surfaces would significantly influence the excess pore water pressure distribution along the depth. Once the ground surface has stronger permeability than the bottom surface, the excess pore water pressure near the ground would dissipate faster than that in other places. In addition, the excess pore water on the drainage boundary decreases with time, which is an important difference between continuous drainage boundary and Terzaghi boundary.

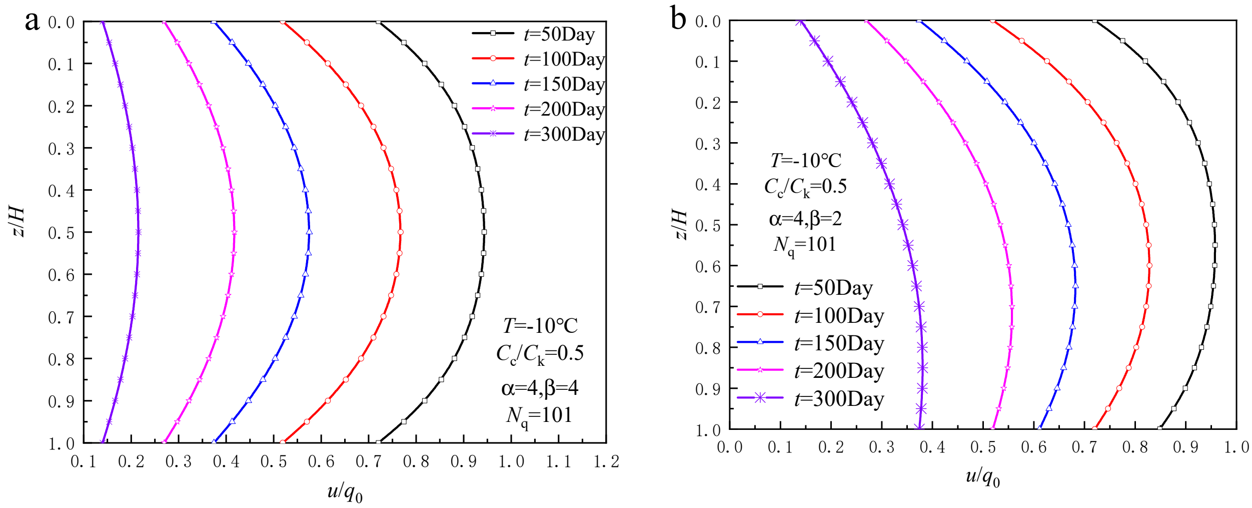

Figure 6. Influence of the time factor: (**a**) the distribution of excess pore water pressure when $\alpha = \beta$, and (**b**) the distribution of excess pore water pressure when $\alpha \neq \beta$.

5.4. Influence of C_c/C_k

The influence of $C_\mathrm{c}/C_\mathrm{k}$ on the excess pore water and degree of the consolidation is illustrated in Figure 7. Both excess pore water pressure and settlement of the soil would decrease with the increase of $C_\mathrm{c}/C_\mathrm{k}$. According to Equation (9), the increase of permeability coefficient k_v originates from the increase of $C_\mathrm{c}/C_\mathrm{k}$. However, the compress coefficient of the soil m_v would not change with the increase of $C_\mathrm{c}/C_\mathrm{k}$. Therefore, the increase of the $C_\mathrm{c}/C_\mathrm{k}$ can only result in the increase of the permeability coefficient, that accelerated soil consolidation.

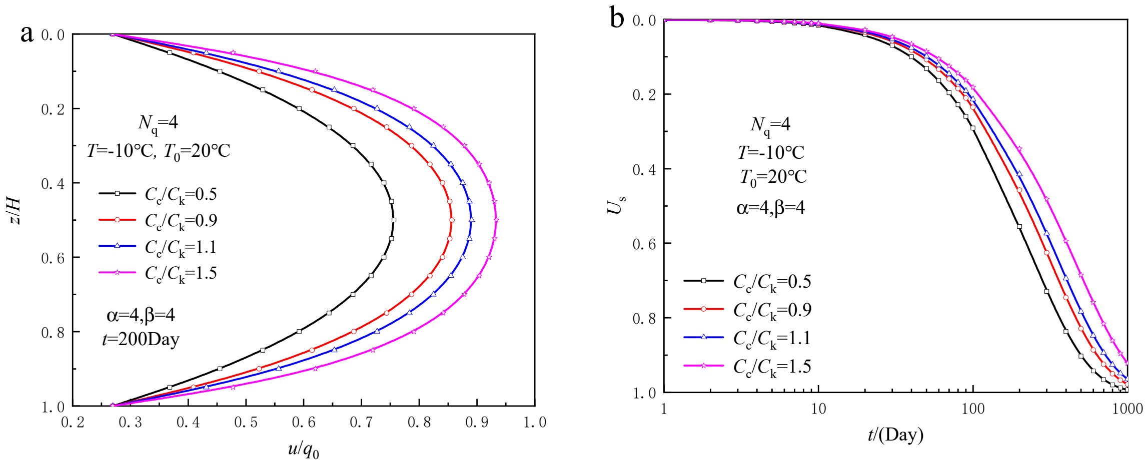

Figure 7. Influence of the pile of $C_\mathrm{c}/C_\mathrm{k}$: (**a**) the distribution of excess pore water pressure, and (**b**) the distribution of the degree of the consolidation defined by settlement.

5.5. Influence of Interface Parameter α and β

As is shown in Figure 8, the excess pore water pressure would dissipate dramatically over the time. The rate of the soil consolidation settlement increases with the increase of the interface parameter. When $\alpha = \beta$, the maximum of the excess pore water is in the middle of the soil depth. If the interface parameters α and β are different, the maximum of excess pore water pressure would be found close to the drainage boundary with the larger interface parameters.

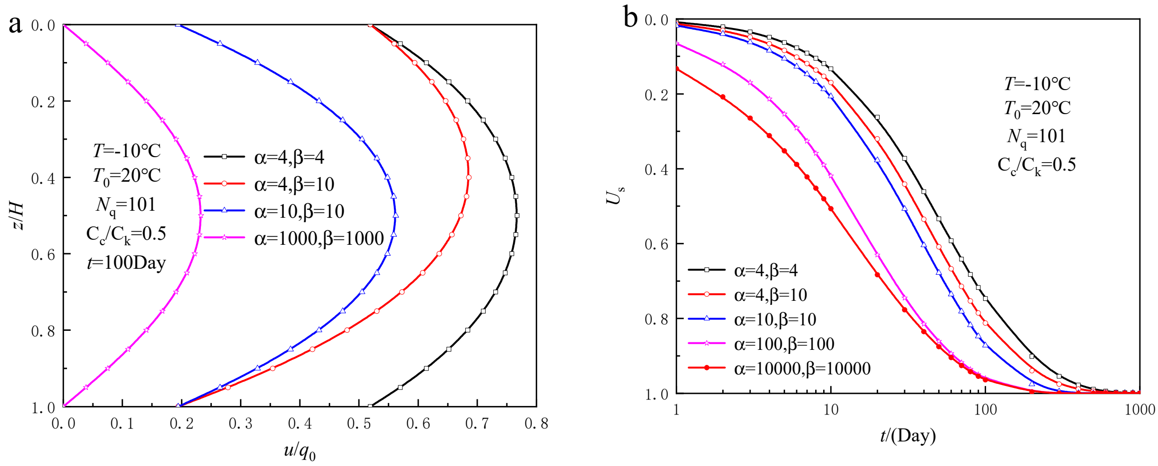

Figure 8. Influence of the interface parameters: (**a**) the distribution of excess pore water pressure, and (**b**) the distribution of the degree of the consolidation defined by settlement.

6. Conclusions

In this paper, a one-dimensional nonlinear consolidation solution considering the thermal effect is derived. The main findings can be concluded as follows:

(1) The temperature has a greater effect on the dissipation of excess pore water pressure. As the temperature increases, the excess pore water pressure would dissipate faster. The soil settlement would decrease with the decrease in temperature in cold regions. That is because the decrease in temperature would make the compressibility index and the permeability of the soil decrease.

(2) When $C_c/C_k > 1$ the consolidation rate would increase with the increase in the ratio of final effective stress to the initial effective stress. It is interesting to find that when $C_c/C_k < 1$, the change of the dissipation of excess pore water pressure is the opposite to that when $C_c/C_k > 1$. The larger N_q is, the faster the excess pore water would be dissipated.

Author Contributions: Conceptualization, Z.W. (Zongqin Wang) and W.W.; methodology, P.Z.; software, Z.W. (Zongqin Wang); validation, Z.W. (Zongqin Wang), Z.W. (Zuodong Wang) and P.Z.; formal analysis, Z.W. (Zuodong Wang); investigation, Z.W. (Zongqin Wang); resources, W.W.; data curation, M.W.; writing—original draft preparation, Z.W. (Zongqin Wang); writing—review and editing, P.Z.; visualization, P.Z.; supervision, R.X.; project administration, Z.W. (Zongqin Wang) and W.W.; funding acquisition, W.W. All authors have read and agreed to the published version of the manuscript.

Funding: This research was funded by National Natural Science Foundation of China, grant number No. 52178371, the Outstanding Youth Project of Natural Science Foundation of Zhejiang Province, grant number No. LR21E080005, the Engineering Research Center of Rock-Soil Drilling & Excavation and Protection, Ministry of Education, grant number No. 202203, and the Fundamental Research Founds for National University, grant number No. CUGDCJJ202207.

Institutional Review Board Statement: Not applicable.

Informed Consent Statement: Not applicable.

Data Availability Statement: The data presented in this study are available on request from the corresponding author.

Conflicts of Interest: The authors declare no conflict of interest.

References

1. Krishnaiah, S.; Singh, D. Determination of influence of various parameters on thermal properties of soils. *Int. Commun. Heat Mass Transfer.* **2003**, *30*, 861–870. [CrossRef]
2. Abuel-Naga, H.M.; Bergado, D.T.; Bouazza, A.; Pender, M.J. Thermal conductivity of soft Bangkok clay from laboratory and field measurements. *Eng. Geol.* **2009**, *105*, 211–219. [CrossRef]
3. Li, H.; Nagano, K.; Lai, Y. Heat transfer of a horizontal spiral heat exchanger under groundwater advection. *Int. Commun. Heat Mass Transfer.* **2012**, *55*, 6819–6831. [CrossRef]
4. Karvien, H.; Aleni, A.H.; Salminen, P.; Minav, T.; Vilave, P. Thermal efficiency and material properties of friction stir channelling applied to aluminium alloy AA5083. *Energies* **2019**, *12*, 1549. [CrossRef]
5. Nocera, F.; Caponetto, R.; Giuffrida, G.; Detommaso, M. Energetic retrofit strategies for traditional sicilian wine cellars: A case study. *Energies* **2020**, *13*, 3237. [CrossRef]
6. Levy, A.; Sorek, S.; Ben-Dor, G.; Bear, J. Evolution of the balance equations in saturated thermoelastic porous media following abrupt simultaneous changes in pressure and temperature. *Transp. Porous Med.* **1995**, *21*, 241–268. [CrossRef]
7. Nguyen, T.S.; Selvadurai, A.P.S. Coupled thermal-mechanical-hydrological behaviour of sparsely fractured rock: Implications for nuclear fuel waste disposal. *Int. J. Rock Mech. Min. Sci.* **1995**, *32*, 465–479. [CrossRef]
8. Wang, Y.; Papamichos, E. Thermal effects on fluid flow and hydraulic fracturing from wellbore and cavities in low-permeability formations. *Int. J. Numer. Anal. Methods Geomech.* **1999**, *23*, 1819–1834. [CrossRef]
9. Paaswell, R.E. Temperature effects on clay soil consolidation. *Soil Mech. Found. Div. J.* **1967**, *93*, 9–21. [CrossRef]
10. Drnevich, P.V.; Tidfors, M.; Sällfors, G. Temperature Effect on Preconsolidation Pressure. *Geotech. Test. J.* **1989**, *12*, 5. [CrossRef]
11. Booker, J.R.; Savvidou, C. Consolidation around a spherical heat source. *Int. J. Soils Struct.* **1984**, *20*, 1079–1090. [CrossRef]
12. Booker, J.R.; Savvidou, C. Consolidation around a point heat source. *Int. J. Numer. Anal. Methods Geomech.* **1985**, *9*, 173–184. [CrossRef]
13. Savvidou, C.; Booker, J.R. Consolidation around a heat source buried deep in a porous thermoelastic medium with anisotropic flow properties. *Int. J. Numer. Anal. Methods Geomech.* **1989**, *13*, 75–90. [CrossRef]
14. Bai, M.; Abousleiman, Y. Thermoporoelastic coupling with application to consolidation. *Int. J. Numer. Anal. Methods Geomech.* **1997**, *21*, 121–132. [CrossRef]
15. Abuel-Naga, H.M.; Bergado, D.T.; Chaiprakaikeow, S. Innovative thermal technique for enhancing the performance of prefabricated vertical drain during the preloading process. *Geotext. Geomembr.* **2006**, *24*, 359–370. [CrossRef]
16. Pothiraksanon, C.; Bergado, D.T.; Abuel-Naga, H.M. Full scale embankment consolidation test using prefabricated vertical thermal drains. *Soils Found.* **2010**, *50*, 599–608. [CrossRef]
17. Artidteang, S.; Bergado, D.T.; Saowapakpiboon, J.; Teerachaikulpanich, N.; Kumar, A. Enhancement of efficiency of prefabricated vertical drains using surcharge, vacuum and heat preloading. *Geosynth. Int.* **2011**, *18*, 35–47. [CrossRef]
18. Cekerevac, C.; Laloui, L. Experimental study of thermal effects on the mechanical behaviour of a clay. *Int. J. Numer. Anal. Methods Geomech.* **2004**, *28*, 209–228. [CrossRef]
19. Blond, E.; Schmitt, N.; Hild, F. Response study of thermal effects on the mechanical behaviour of a clay. *Int. J. Numer. Anal. Methods Geomech.* **2003**, *27*, 883–904. [CrossRef]
20. Bai, B. Thermal consolidation of layered porous half-space to variable thermal loading. *Appl. Math. Mech.* **2006**, *27*, 1531–1539. [CrossRef]
21. Chen, G.J.; Ledesma, A. Coupled solution of heat and moisture flow in unsaturated clay barriers in repository geometry. *Int. J. Numer. Anal. Methods Geomech.* **2007**, *31*, 1045–1065. [CrossRef]
22. Yu, L.; Chen, G.J. transient heat and moisture flow around heat source buried in an unsaturated half space. *Transp. Porous Media* **2009**, *78*, 233–257. [CrossRef]
23. Ai, Z.Y.; Wang, L.J. Axisymmetric thermal consolidation of multilayered porous thermoelastic media due to a heat source. *Int. J. Numer. Anal. Methods Geomech.* **2015**, *39*, 1912–1931. [CrossRef]
24. Terzaghi, K. *Erdbaumechanik and Bodenphysikalischer Grundlage*; Franz Deuticke: Leipzig, Germany, 1925.
25. Davis, E.H.; Raymond, G.P. A non-linear theory of consolidation. *Geotechnique* **1965**, *15*, 161–173. [CrossRef]
26. Chen, D.Q.; Lou, J.H.; Liu, X.L.; Mi, D.C.; Xu, W.W. Improved double-layer soil consolidation theory and its application in marine soft soil engineering. *J. Mar. Sci. Eng.* **2019**, *7*, 156. [CrossRef]
27. Xie, K.H.; Xie, X.Y.; Jiang, W. A study on one-dimensional nonlieaner consolidation of double-layered soil. *Conput. Geosci.* **2002**, *29*, 151–168.
28. Xie, K.H.; Xia, C.Q.; An, R.; Ying, H.W.; Wu, H. A study on one-dimensional consolidation of layered structured soil. *Int. J. Numer. Anal. Methods Geomech.* **2016**, *40*, 426–431. [CrossRef]
29. Kim, P.; Kim, H.S.; Pak, C.U.; Paek, C.H.; Ri, G.H.; Myong, H.B. Analytical solution for one-dimensional nonlinear consolidation of saturated multi-layered soil under time-dependent loading. *J. Ocean Eng. Sci.* **2021**, *6*, 21–29. [CrossRef]
30. Mesri, G.; Rokhsar, A. Theory of consolidation for clays. *J. Geotech. Eng.* **1974**, *100*, 1090–1093.
31. Duncan, J.M. Limitations of conventional analysis of consolidation settelement. *J. Geotech. Eng.* **1993**, *119*, 1333–1359. [CrossRef]
32. Chen, R.P.; Zhou, W.H.; Zhang, J.C.; Fan, Z.C. One-dimensional nonlinear consolidation of multi-layered soil by differential quadrature method. *Conput. Geotech.* **2005**, *32*, 358–369. [CrossRef]

33. Hu, A.F.; Xia, C.Q.; Li, C.X.; Xie, K.H. Nonlinear consolidation analysis of Natural Structures Clays under time-dependent loading. *Inter. J. Geomech.* **2018**, *18*, 04017140. [CrossRef]
34. Gray, H. Simultaneous consolidation of contiguous layers of unlike compressible soils. *T. Am. Soc. Civ. Eng.* **1945**, *110*, 1327–1356.
35. Schiffman, R.L.; Stein, J.R. One-dimensional consolidation of layered systems. *J. Soil Mech. Found. Div.* **1970**, *96*, 1499–1504. [CrossRef]
36. Mesri, G. One-dimensional consolidation of a clay layer with impeded drainage boundaries. *Water Resour. Res.* **1973**, *9*, 1090–1093. [CrossRef]
37. Mei, G.X.; Chen, Q.M. Solution of Terzaghi one-dimensional consolidation equation with general boundary conditions. *J. Cent. South Univ.* **2013**, *20*, 2239–2244. [CrossRef]
38. Mei, G.X.; Lok, T.M.H.; Xia, J.; Wu, S.S. One-dimensional consolidation with asymmetrical exponential drainage boundary. *Geomech. Eng.* **2014**, *6*, 47–63. [CrossRef]
39. Zhou, W.H.; Zhao, L.S.; Garg, A.; Yuen, K.V. Generalized analytical solution for the consolidation of unsaturated soil under partially permeable boundary conditions. *Int. J. Geomech.* **2017**, *17*, 04017048. [CrossRef]
40. Wang, L.; Sun, D.A.; Qin, A.F. Semi-analytical solution to one-dimensional consolidation for unsaturated soils with exponentially time-growing drainage boundary conditions. *Int. J. Geomech.* **2018**, *18*, 04017144. [CrossRef]
41. Huang, M.H.; Li, J.C. Generalized analytical solution for 2D plane strain consolidation of unsaturated soil with time-dependent drainage boundaries. *Comput. Geotech.* **2018**, *103*, 218–228. [CrossRef]
42. Zong, M.F.; Tian, Y.; Liang, R.Z.; Wu, W.B.; Xu, M.J.; Mei, G.X. One-dimensional nonlinear consolidation analysis of soil with continuous drainage boundary. *J. Cent. South Univ.* **2022**, *29*, 270–281. [CrossRef]
43. Quan, L.; Deng, Y.B.; Chen, F. One-dimensional non-linear consolidation theory of soft ground coupled with thermal effect. *Proc. Inst. Civ. Eng.-Ground Improv.* **2019**, *172*, 138–145. [CrossRef]
44. Eriksson, L.G. Temperature effects on consolidation properties of sulphide clays. *Balkema Publ.* **1989**, *3*, 2087–2090.
45. Wang, Y.Y. *Geotechnical Test and Soil Mechanics Guidance*; Yellow River Water Conservancy Press: Zhengzhou, China, 2004.
46. Guo, P.H.; Liu, Y.X.; Hu, Y. The regional temperature effects on consolidation of saturated clays. *Goal Geol. Explor.* **2012**, *40*, 62–66. (In Chinese)
47. Lekha, K.R.; Krishnaswamy, N.R.; Basak, P. Consolidation of clays for variable permeability and compressibility. *J. Geotech. Geoenviron. Eng.* **2003**, *129*, 1001–1009. [CrossRef]
48. Lin, C.N.; Li, H.P.; Zhang, J.B.; Zhu, Y.L. Relationship among elastic modulus, temperature and stain rate of frozen medium under static loading. *Chin. J. Rock. Mech. Eng.* **2003**, *22*, 2700–2702. (In Chinese)